（様式５）(Style5)

<h1 style="text-align:center">学位論文全文に代わる要約
Extended Summary in Lieu of Dissertation</h1>

氏名：
Name   Moses Wazingwa Munthali

学位論文題目： Title of Dissertation	Studies on Cation Adsorption Properties of Zeolites and the Development of Radioactive Decontamination Method using Zeolites （ゼオライトの陽イオン吸着特性及びゼオライトを用いた放射能除染法の開発に関する研究）

学位論文要約：
Dissertation Summary

1.0 Background

Significant amounts of radioactive Cs and Sr in unacceptable levels have contaminated the environment through anthropogenic activities such as mining, nuclear weapons testing, discharges from nuclear power plants or ships, and accidental release like Fukushima nuclear power plant accident in 2011 (Illman, 1993; Wilson, 1997; Dyer, 2000; Zheng et al., 2012). After the Fukushima accident, soils of Fukushima were characterized as contaminated soils. Radioactive ^{90}Sr and ^{137}Cs which are beta and strong beta-gamma emitters respectively are produced by nuclear fission and are un-biodegradable with half-lives of 29 and 30 years respectively causing shielding challenges (Tiwari et al., 2006). This means the contaminated soils have to be kept for at least 100 years in designated repositories. Implying the radioactive contaminated agricultural soils would no longer be available for agricultural use for at least 100 years. Furthermore, Cs^+ and Sr^{2+} are easily engaged into K^+ and Ca^{2+} metabolic cycles respectively due to their high biological availability potential of accumulating in plants and animals. Once radioactive Cs and Sr are in human body through food chain pathways, they have high risk of carcinogenic effect i.e. skin cancer and leukemia respectively (National Research Council, 1981; Irwin et al., 1997).

In Japan, after the Fukushima accident, it is calculated that 15750 acres of paddy rice and 5000 acres of upland fields excluding forest soils in Fukushima alone were characterized by radioactive Cs concentrations of above the threshold of 5000 Bq kg^{-1} in contaminated soils (IAEA, 2011). Radioactive contamination is likely to continue through mining activities, authorized discharges and possible future nuclear accidents and wars. Hence, in order to reduce the risk of radioactivity hazardous in environment and to human beings, it is vital to remove radionuclides from contaminated soil and water. Currently, several different technologies have been developed for use in the removal of radionuclides from nuclear wastes that include: precipitation, ion exchange, phytoextraction, reverse

osmosis, electrodialysis, vacuum evaporation, solvent extraction and carbon adsorption (Erdem et al., 2004; Alvarez-Ayuso et al., 2003; Semmens and Martin, 1988). However, adsorption and ion-exchange work rather well and are commonly used because of their ease of use, simple and robust design. The only challenge is that the use of ionic-exchange organic adsorbents such as activated carbon and ion-exchange resins cannot be regenerated, are expensive and not feasible for use in small-scale operations or in developing countries where resources may be limited (Gallant and Prakash, 2009). Furthermore, adsorbents used to clean nuclear wastewater and contaminated water bodies generally have to be stored for many years before they are no longer hazardous and are safe for disposal by traditional means.

Recently, there has been a push to find efficient and low-cost adsorbents. Some of the materials considered include peat moss and dead biomass (Babel and Kurniawan 2003; Baily et al., 1999). However, they have in most cases inferior properties such as thermal stability. On the other hand, use of inorganic ion exchangers such as natural clays and zeolites are more promising in the radioactive waste management and remediation of polluted water bodies. They have high cation exchange capacity (CEC), high cation selectivity and specificity, capability of retaining or fixing radionuclides, offer superior chemical stability and possess fairly good radiation and thermal resistance capacities (Abdel Rahman et al., 2011; Tiwari et al., 2006). These characteristics are simply not achievable with organic compound ion-exchangers. Inorganic ion-exchangers can be used to remove both Cs and Sr with a high level of selectivity under a broad pH range. They can operate at acidic pH where protons inhibit ion exchange in alternative technologies such as crystalline silicotitanate (CST).

Currently, in terms of soil radioactive decontamination, there are primarily two methods being used to reduce human exposure to radioactive contamination: a) phytoremediation which uses plants and is primarily very inefficient (i.e. in the Chernobyl accident, only 0.05% of Cs^+ was removed by sunflowers), slow and expensive for it requires incineration facilities (IAEA, 2011; Dushenkov, 2003; Su et al., 2008); b) soil excavation option which involves removal of the radioactive contaminated top soil layer (i.e. 400 ton/ha), keeping the removed contaminated soil for at least 100 years in designated repositories and is very costly with adverse effects on soil biological activities and ecosystem (IAEA, 2011). Recently, synthetic magnetic inorganic adsorbents have shown to be relatively effective with utmost 60% Cs^+ decontamination from contaminated soil (Aono et al., 2013; Maca′sˇek et al., 2002). However, the technology is likely to be very expensive and complicated. Hence, there is an urgent need to develop simple, low cost and effective methods for radioactive decontamination that can also be used by developing countries where resources may be limited. Use of natural zeolites could be one of the best and cheap ways.

Zeolites are well known molecular sieves with different pores/cavities, high cation exchange capacity, strong specific cation adsorption selectivity and high affinity towards specific cations such as Cs^+ and Sr^{2+}. And this makes zeolites to be more effective, selective and superior adsorbents and catalysts for separating specific ions in aqueous system or molecules from air (Bonelli et al., 2000; Abdel-Rahman et al., 2011; Kim, 2003). As such, zeolites are used as adsorbents of cationic elements in the radioactive decontamination process of water and others. Along with the use of zeolites as catalyst, they are utilized to adsorb and remove various cations in aqueous system at a wide range of

aqueous pH (Munthali et al., 2014). Furthermore, negative charges present in the structural frameworks of zeolites are saturated by specific cations to modify their physicochemical and catalytic properties thereby broadening their applications. The efficiency of zeolites in their use is primarily dependent on their pore/cavity sizes and amount of negative charge derived from isomorphous substitution of Si by Al. This means their cation adsorption capacity under different ion coexistence at different pH is likely to vary much. However, the phenomenon is not well understood and how the amount of negative charges are affected at different pH. Therefore, evaluation studies on cation adsorption properties of zeolites and development of radioactive decontamination method using zeolites were done. Adsorption behaviour of H^+, Li^+, Na^+, K^+, Rb^+ and Cs^+ on Li^+, Na^+, K^+, Rb^+ and Cs^+-saturated Linde-type A, Na-P1, mordenite, X type and Y type zeolites were evaluated at different pH−pM, where pH−pM is equal to log $\{(M^+)/(H^+)\}$ and M^+ represents either Li^+, Na^+, K^+, Rb^+ or Cs^+. The cationic adsorption selectivity sequences of the zeolites were also determined. Furthermore, the radioactive decontamination methods were developed for the decontamination of radioactive Cs^+ and Sr^{2+} from contaminated water and soil using the zeolites.

2.0 Materials and Methods

Linde-type A, Na-P1, mordenite, faujasite X and faujasite Y zeolites with different Si/Al ratios, crystal structures and amount of charge densities were used in this study. All standard analytical chemical reagents and zeolite samples used in this study were purchased from Wako Chemicals Ltd, Japan except for Na-P1 zeolite sample which was synthesized in this study.

2.1 Preparation of Li^+, Na^+, K^+, Rb^+ and Cs^+-Saturated Zeolites

In respective 250 mL centrifuge bottle, 10 g of each added zeolite samples were washed five times with 150 mL of 1 M chloride solutions of Li^+, K^+, Rb^+ or Cs^+ to saturate the zeolites with the alkali metal cation. Thereafter, the contents were washed twice with 150 mL of water and then washed once with 100 mL of acetone, air-dried, and used as samples. Cations contained in the samples were exchangeable alkali metal cation, and free Li^+, K^+, Rb^+ or Cs^+ as chloride salt. The sum of exchangeable and free Li^+, K^+, Rb^+ or Cs^+ content of the sample (hereafter Li^+, K^+, Rb^+ or Cs^+ content) were determined by washing 1 g of the sample with 30 mL of 1 M NH_4Cl in a 50 mL centrifuge bottle for seven times. Water content of the samples was determined by heating at 105 °C for 3 h. The content of Si and Al of the samples was determined after dissolution with hydrofluoric acid.

2.2 Determination of CEC of Zeolites at Different pH

One gram of Li^+, Na^+, K^+, Rb^+ or Cs^+ saturated Linde-type A, Na-P1, mordenite, faujasite X or faujasite Y was put into a 250 mL centrifuge bottle, and 200 mL of 0 to 7.5 mM HCl solution was added. To obtain CEC values at higher pH, 200 mL of 0 to 5 mM LiOH, KOH, RbOH or CsOH solution was added instead of HCl solution. The mixture was shaken for 3 h at 25 ± 0.5 °C, centrifuged at 2000 g, and the concentration of the alkali metal and pH of the supernatant were

measured. Preliminary experiments revealed that the Na^+ concentration and pH of the supernatant became constant within 3 h, and the measured Li^+, K^+, Rb^+ or Cs^+ concentration and pH are hereafter referred to as equilibrium Li^+, K^+, Rb^+ or Cs^+ concentration and equilibrium pH, respectively. The CEC (the amount of alkali metal cation retention) of the respective samples were simply calculated from the difference between the content of each alkali metal cation of the samples and the amount of the alkali metal cation in the supernatant solution. Also Al and Si concentrations were measured in the supernatant to check the dissolution of zeolite samples. The quantifications of the metals were done by using atomic absorption spectrophotometer (Hitachi Z-5000). Powder X-ray diffraction patterns of the samples before and after the CEC determination were obtained with a Rigaku Ultima IV X-ray diffractometer with Cu-Kα radiation generated at 40 kV and 40 mA, between 3-60° of 2θ angles with a sampling width of 0.02° and a scanning rate of 2° min^{-1} Interms of decontamination of radioactive Cs and Sr from water, 30 mL of a mixed solution containing up to 15 mg L^{-1} of non-radioactive Cs^+ or Sr^+ and up to 0.50 M of Na^+ or K^+ was mixed with 0.5 g of Linde-type A, Na-P1, faujasite X, faujasite Y and mordenite. The reaction time was 1 h. In case of soil decontamination, zeolites were coexisted with contaminated soil in the presence of the extracting salt solution. Different variables such as solid/solution ratio, time, concentration, pH, zeolite species and method of coexistence were evaluated.

2.3 Cs^+ and Sr^{2+} Decontamination experiments from water

Preparation of Na^+-saturated samples of Linde-type A, Na-P1, faujasite X, faujasite Y and mordenite was done by washing the zeolites with a 1 M $NaNO_3$ solution, followed by washing with water. The prepared zeolite samples had the amounts of isomorphous substitution of 5.56 mmol g^{-1} for Linde-type A, 4.40 mmol g^{-1} for faujasite X, 4.29 mmol g^{-1} for Na-P1, 2.40 mmol g^{-1} in faujasite Y, and 1.76 mmol g^{-1} for mordenite. Each 0.5 g of the Na^+-saturated zeolite was put into a 50 mL centrifuge bottle, and a 30 mL of nitrate solution containing 0 to 15 mg L^{-1} Cs^+ or Sr^{2+} (Cs^+: 0 to 113 μM, Sr^{2+}: 0 to 171 μM) was added. In the solution, 0.05, 0.10 or 0.50 M of $NaNO_3$ or KNO_3 coexisted. We must note here that the amount of positive charge of Cs^+ and Sr^{2+} added was less than 1.2% of the negative charge of the zeolites. The bottle was shaken in a water bath for 1 h at a constant temperature of 25 ± 0.2 °C, and centrifuged at 2000 g for 10 min. The reaction time of 1 h was determined in the preliminary experiments. The concentrations of Cs^+ and Sr^{2+} in the supernatant were measured by an atomic absorption spectrophotometer (AAS: Hitachi Z-5000), and the amounts of adsorption of Cs^+ and Sr^{2+} were calculated from the difference between their initial and final concentrations.

2.4 Calculation of distribution coefficient (K_d)

Another experiment was set up similar to above with a fixed initial Cs^+ and Sr^{2+} concentration of 10 mg L^{-1} under the same temperature of 25 °C. The data from this experiment was used to calculate a distribution coefficient (K_d) (Sangvanich et al., 2010) and adsorption ratio. The distribution coefficient (K_d) was calculated by the following equation.

$$K_d \ (mL \ g^{-1}) = [(A_i - A_f) / A_f] \times V/M \qquad (1)$$

Where A_i is initial concentration of Cs^+ or Sr^{2+} (mol L^{-1}), A_f is equilibrium concentration of Cs^+ or Sr^{2+}

(mol L^{-1}), V is volume of solution phase (mL) and M is mass of the adsorbent (g) (El-Naggar et al., 2008).

2.5 Development of radioactive decontamination method using vermiculite

Simulated decontamination experiments of Cs- and Sr-contaminated soils were carried out by using a vermiculite sample (>150 μm). The CEC of the vermiculite sample was measured by the method of Barshad and Kishk (Barshad and Kishk, 1970). The vermiculite sample was washed with water, air-dried, and CsNO$_3$ or Sr(NO$_3$)$_2$ solution was added to obtain Cs- or Sr-retaining vermiculite: the amount of retention of Cs and Sr was set to 60 mg kg^{-1}. The Cs- and Sr-retaining vermiculites were washed with water, air-dried, and used as simulated Cs- and Sr-contaminated soils. Two methods (direct and indirect) were used in the removal of Cs from the contaminated soils. Both methods involved the coexistence of vermiculite and mordenite in the presence of the extracting solutions; tea bag method and direct method. Then 2 g of the Cs-retaining vermiculite was mixed with 2 g of Na$^+$-saturated mordenite (< 90 μm) in a 250 mL polyethylene bottle, and 60 mL of 0.3 M KCl solution was added. The contents were shaken for 3 h, and vermiculite and mordenite were separated each other by wet sieving using a 105 μm sieve. Different factors were also evaluated such as reaction time, extraction solution types, solid to solution ratio and etc. The same experiment was also carried out by using the Sr-retaining vermiculite and Na$^+$-saturated Linde-type A (< 90 μm). Blank runs without the zeolites were also conducted. The contents of Cs of Cs-retaining vermiculite and Sr of Sr-retaining vermiculites before and after the decontamination experiment were determined by dissolving 1 g of the vermiculites with 30 mL of 3 M HNO$_3$ at 100 ^{o}C for 3 h and subsequent determination of Cs and Sr by AAS.

2.6 Evaluation of radioactive decontamination method using contaminated soil

Different types of Fukushima soils were used in the Cs decontamination experiments. The method was modified by using various extracting salt solutions that included 0.3M (NH$_4$)$_2$C$_2$O$_4$, 0.3M NH$_4$NO$_3$, 0.3M KCl, 0.3M Mg(NO$_3$)$_2$, Fe(NO$_3$)$_3$, tap H$_2$O and a mixture of 0.1M KOH and 0.1M K$_4$P$_2$O$_7$ in the ratio of 1:1. Direct and indirect methods were used in the decontamination of Cs from the contaminated soils. Under direct method, the soils were used either a whole or as fractionates of large and small particles of adsorbent and desorbent. Powder mordenite was used to decontaminate large soil particles while large mordenite was used to decontaminate small soil particles. Large mordenite (> 250 μm) was also used to decontaminate the entire soil; the soil was wet ground into fine particles that could pass through the 250 μm sieve. The mixing of soil, extracting solution and mordenite was done by rotational, horizontal shaking and stirring by magnetic stirrer.

3.0 Results and Discussion

3.1 Structural Stability of Zeolites with CEC Measurement

The determination of CEC of zeolites was conducted in pH range of moderately acidic to moderately alkaline, and so we checked the stability of zeolites i.e., if they underwent dissolution or not in aqueous solution. We analyzed XRD patterns for each treated zeolite sample after CEC measurement, and the results for the water (lower) and highest HCl concentration (upper) treated samples are given in Figure 1. We also quantified the percentage Si and Al dissolved from zeolites structural frameworks and the amounts were less than 2% for Si and 0.5% Al. The dissolution was very minimal possibly because the reaction time was only 3 h. Analysis of XRD patterns in Figure 1 of all zeolite samples indicated that there was neither change in their structures nor formation of new materials. Comparison of the XRD patterns indicated that there was an increase in peak intensities of most samples after CEC measurement.
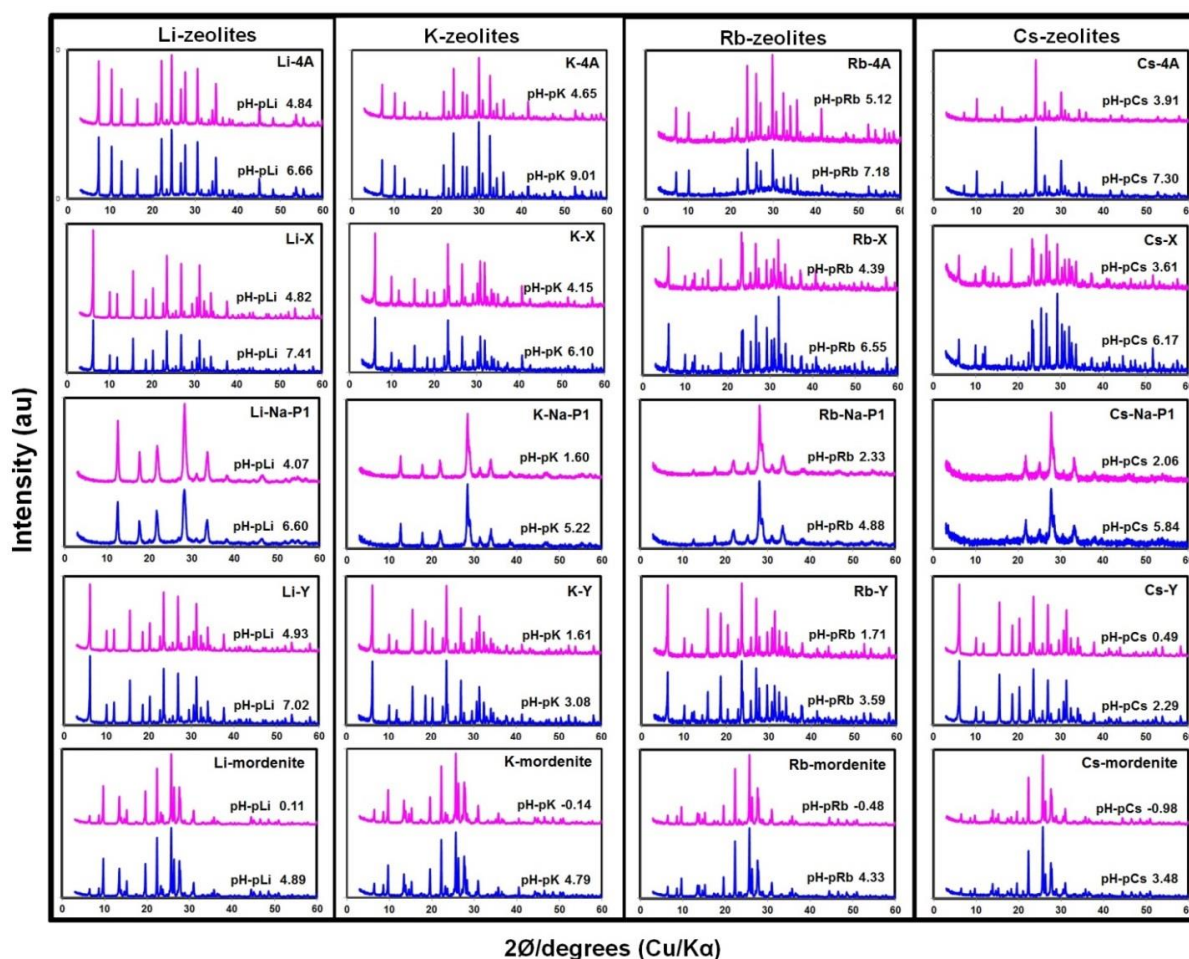

Figure 1. XRD patterns of zeolites after CEC measurement.

3.2 Effect of pH-pM on CEC Measurement of zeolites

In this experiment, CEC or the amount of retention of an alkali metal cation of a zeolite is affected not only by pH, but also by the concentration of the alkali metal cation in the solution phase. On one hand, CEC of clays in a monovalent cation system is known to be dependent on the value of

pH−pM (M: activity of Na$^+$ or NH$_4^+$), and this means CEC is dependent on the ratio of activities of the monovalent cation to H$^+$. Therefore we plotted measured CEC values against pH−pM (M: activity of Li$^+$, K$^+$, Rb$^+$ or Cs$^+$), and the plots are shown in Figure 2. Generally, the results indicated that with decreasing pH−pM, the amounts of the alkali metals retention decreased due to the adsorption of H$^+$ via cation exchange reaction. The adsorption selectivity of H$^+$ to the zeolites had a negative correlation with the Si/Al ratio of the zeolites. Although each zeolite has a constant amount of negative charge, the amount of Na$^+$ adsorption of each zeolite decreased drastically at low pH−pNa values, where pH−pM is equal to log$\{$(M$^+$)/(H$^+$)$\}$. By using the plot of the amount of M$^+$ adsorption versus pH−pM, an index of the H$^+$ selectivity, which is similar to pKa of acids, of each zeolite was estimated, and the index tended to increase with decreasing Si/Al ratio of zeolites. These indicate that zeolites with lower Si/Al and higher negative charge density have higher H$^+$ adsorption selectivity, and in fact, such a zeolite species (4A and X) adsorbed considerable amount of H$^+$ even at weakly alkaline pH region. Furthermore, in each zeolite species, Cs$^+$-saturated zeolite showed the lowest H$^+$ selectivity, and this suggested that Cs$^+$ had the strongest adsorption energy in the alkali metal cations. The adsorption of H$^+$ was strongly affected by diameter and hydration energy of the alkali metal cations, and also affected by framework type and Si/Al ratio of the zeolites. The adsorption of H$^+$ to zeolites decreases the amount of cation retention other than H$^+$, and may cause the elution of Si and Al into aqueous solution.

The reason why CEC decreased with decrease in pH-pM can be well explained if we look at the specific Brönsted and Lewis acid-base sites exist in zeolite micropores (Almutairi et al., 2013; Serykh, 2005). Considering the Lewis acid-base sites, after a proton is adsorbed through ion exchange with Na$^+$, the proton acts as a Lewis acid while the O between Si−O−Al acts as a Lewis base. Then the O gives lone pair electrons to the proton which results into a negative charge neutralization due to the formation of covalent bonding between the O and the proton (Santen and Neurock, 2009). The formed covalent bonding results into neutral charge and a loss of negative charge in zeolite. The covalent bonding is much stronger than the ionic bonding formed by Na$^+$ cation in balancing up the negative charge.
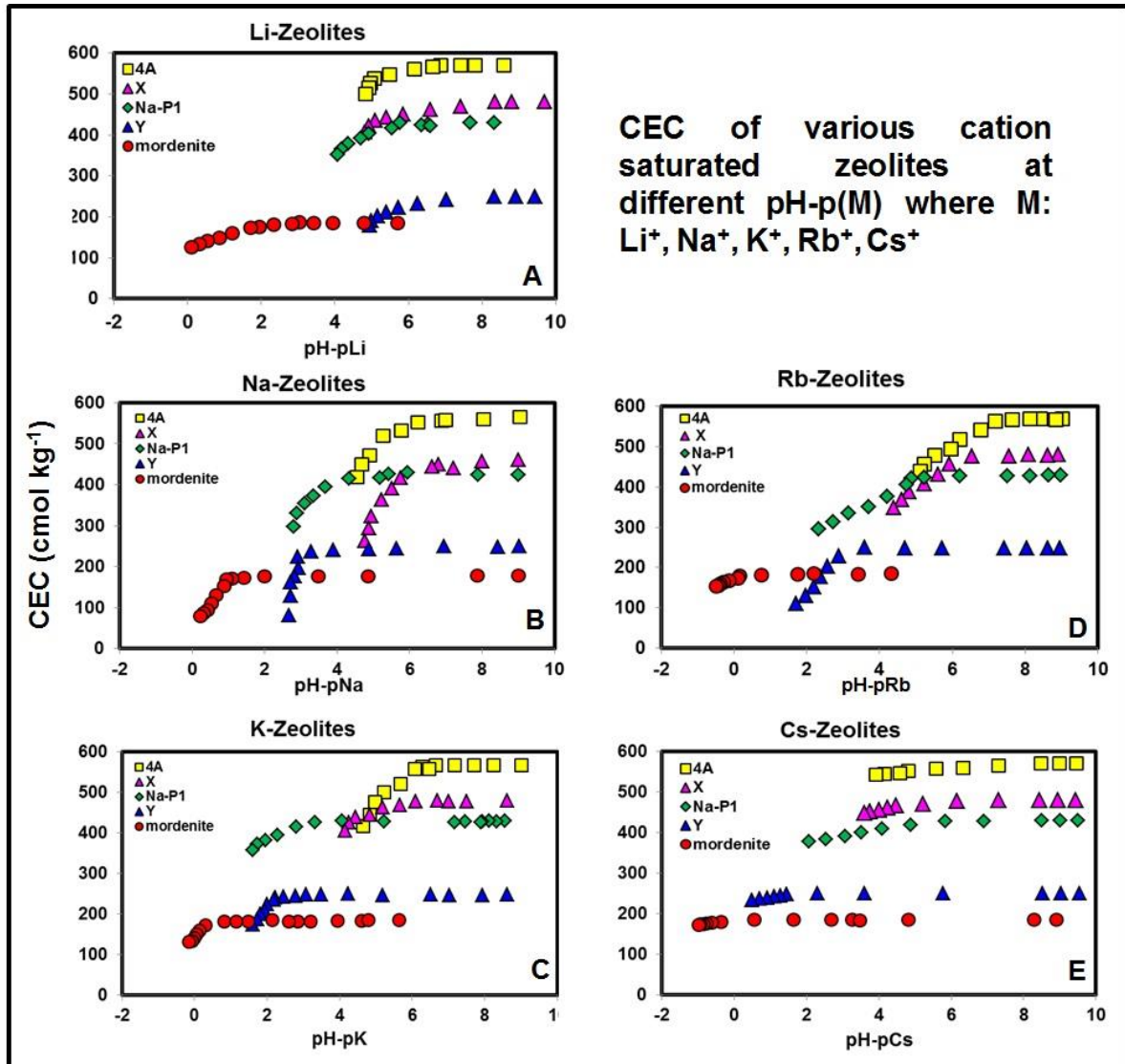
*Figure 2.*Change in CEC of zeolites with pH−pM. A: Li-zeolites, B: K-zeolites, C: Rb-zeolites, D: Cs-zeolites. cmol in the unit of CEC is centimole.

3.3 Effect of Cation and Zeolite Species on Proton Adsorption

The degree of H^+ adsorption selectivity varied greatly and was influenced by alkali metal cation species and by zeolite species (Figure 2). We compared the $(pH-pM)_{90}$ values for each cation saturated zeolites and the results are summarized in Table 1. The results indicated that $(pH-pM)_{90}$ values were different among alkali metal cation species and also among zeolite species. In general, Cs^+ saturated zeolites had the lowest $(pH-pM)_{90}$ value, and this indicated that H^+ adsorption selectivity was lowest for the Cs^+ saturated zeolite. In other words, among alkali metal cations, Cs^+ had the highest adsorption selectivity toward zeolites. This result is partly explained by the hydration diameter sequence order of the alkali metal cations, but the other four cations are not followed this order: for

example, Rb^+ saturated zeolites had higher $(pH-pM)_{90}$ values than K^+ saturated zeolites except for mordenite.

Table 1. Effect of saturated cations in zeolites on pH−pM$_{90}$ (M: Li$^+$, Na$^+$, K$^+$, Rb$^+$, Cs$^+$).

Saturated zeolite	pH−pLi$_{90}$	pH-pNa[*]	pH−pK$_{90}$	pH−pRb$_{90}$	pH−pCs$_{90}$
Linde-type A	5.61	5.38	5.64	6.23	3.80
X	5.90	5.75	4.30	5.59	3.21
Na-P1	4.34	3.64	2.47	4.42	2.53
Y	4.79	3.06	2.02	2.71	0.57
Mordenite	0.51	0.92	0.18	-0.33	-0.42

By using the data in Table 1, for each saturation cation type, the H^+ adsorption selectivity sequence among the zeolite species is summarized in Table 2. In K^+-, Rb^+- and Cs^+-types, Linde-type A had the greatest H^+ adsorption selectivity, while in case of Li^+- and Na^+-types, the strongest H^+ adsorption selectivity was in faujasite X.   On one hand, in all saturation cation species, mordenite had the lowest H^+ adsorption selectivity. The H^+ adsorption selectivity sequence of the zeolite species is also summarized in Table 3, in which the effect of the saturation cation species was evaluated in each zeolite species. As has been described earlier, in most zeolite species Cs^+-type showed the lowest H^+ adsorption selectivity. The positions of the other saturation cation types at the sequences were varied, but the sequences of faujasite X and faujasite Y were identical. This indicated that H^+ and alkali metal cations selectivity sequences were affected by the type of zeolite framework. The proton Adsorption Selectivity of Zeolites was affected by the Si/Al Ratio of zeolites, amount of charge density in zeolites, nature of adsorbing cations and pore sizes of zeolites. Usually the variations in Si−O−Al angles and bond lengths, differences in crystal structures and amounts of Si−O−Si or Si−O−Al affect the ion adsorptions of H^+, Li^+, Na^+, K^+, Rb^+ and Cs^+ on surface charge sites within and among zeolites (Noda et al., 2008). The presence of Si−O−Si and Si−O−Al links determines the occurrence of a number of acidic sites, and the adsorption of H^+ to zeolites leads to the occurrence of Brönsted acid site (Katada et al., 2009). Adsorption of Li^+, Na^+, K^+, Rb^+ and Cs^+ on negative charge sites and the surrounding atoms affects the degree of Lewis basic strength differently (Sastre et al., 2010; Katada et al., 2009) which in turn affects the H^+ selectivity. The attachment of Li^+, Na^+, K^+, Rb^+ and Cs^+ as a balancing charge cation in zeolites causes variations in the H^+ selectivity and Lewis acidity (Hiromi and Masakazi, 2000). This explains why the H^+ selectivity was different among Li^+, Na^+, K^+, Rb^+ and Cs^+ saturated zeolites. Furthermore, the difference in the Si/Al ratio among zeolites resulted into variations in the amount of negative charge or cation exchange capacity (CEC) of mordenite (179 cmol kg^{-1}),

Linde-type A (565 cmol kg^{-1}), Na-P1 (429 cmol kg^{-1}), faujasite X (461 cmol kg^{-1}) and faujasite Y (250 cmol kg^{-1}) (Munthali etal., 2014).

Table 2: *Proton adsorption selectivity sequences of zeolites: the effect of zeolite species.*

Saturation Cation	H$^+$ adsorption selectivity sequence
Li$^+$	faujasite X > Linde-type A > faujasite Y > Na-P1 > mordenite
Na$^+$	faujasite X > Linde-type A > Na-P1 > faujasite Y > mordenite
K$^+$	Linde-type A > faujasite X > Na-P1 > faujasite Y > mordenite
Rb$^+$	Linde-type A > faujasite X > Na-P1 > faujasite Y > mordenite
Cs$^+$	Linde-type A > faujasite X > Na-P1 > faujasite Y > mordenite

Table 3: *Proton adsorption selectivity sequences of zeolites: the effect of saturation cation species.*

Zeolite	H$^+$ adsorption selectivity sequence
Linde-type A	Rb$^+$-type > K$^+$-type > Li$^+$-type > Na$^+$-type > Cs$^+$-type
faujasite X	Li$^+$-type > Na$^+$-type > Rb$^+$-type > K$^+$-type > Cs$^+$-type
Na-P1	Rb$^+$-type > Li$^+$-type > Na$^+$-type > Cs$^+$-type > K$^+$-type
faujasite Y	Li$^+$-type > Na$^+$-type > Rb$^+$-type > K$^+$-type > Cs$^+$-type
mordenite	Na$^+$-type > Li$^+$-type > K$^+$-type > Rb$^+$-type > Cs$^+$-type

3.4 Cs$^+$ and Sr^{2+} Decontamination experiments from water

In case of Cs$^+$ and Sr^{2+} adsorption selectivity among the zeolites, mordenite had the highest Cs$^+$ adsorption selectivity, and the selectivity had no correlation to the cation exchange capacity (CEC) of the zeolites. In contrast, Sr^{2+} adsorption selectivity of the zeolites positively correlated with the CEC of the zeolites: Linde-type A with the highest CEC showed the highest adsorption selectivity, and its adsorption rate was more than 99.9% even in the presence of 0.5 M K$^+$. Adsorption selectivity behaviours of Cs$^+$ and Sr^{2+} on Linde-type A, Na-P1, mordenite, X and Y zeolites were greatly depended on variations in structural framework of zeolite species, concentration or activity of electrolytes, and type of coexisting competing cations. The amount and selectivity adsorption

behaviour of Cs^+ in the five zeolites was significantly influenced by differences in pore sizes while for Sr^{2+} it was mainly influenced by variations in CEC amounts of various zeolites. The CEC had little effect on Cs^+ selectivity adsorption behaviour on the various zeolites. The sequential orders of adsorption selectivity behaviours for Cs^+ and Sr^{2+} by various zeolites were different within and among various zeolites under different concentrations of coexisting Na^+ or K^+ in the aqueous solution. The amounts of Cs^+ and Sr^{2+} adsorption by various zeolites were different and depended on amounts of coexisting K^+ or Na^+. In case of the binding energy was strongest for Cs^+ in mordenite and weakest in Linde-type A. While for Sr^{2+} the strongest binding energy was in Linde-type A and X and the lowest was in mordenite and Y. The findings would help to use the appropriate zeolites species for efficient decontamination of Cs^+ and Sr^{2+} under different conditions of radionuclides contaminated aqueous environments with different electrolyte activities and coexisting cations.

3.5 Development of radioactive decontamination method using vermiculite

The results of a simulated soil decontamination experiment using Cs- and Sr-retaining vermiculites indicated that there was generally significant decontamination of Cs^+ and Sr^{2+} from Cs- and Sr-retaining vermiculites respectively due to coexistence with zeolites in the presence of the extracting salt solution. The decontamination rates were affected by different variables that included time and method of shaking, adsorbent type, type of extracting salt solution, particle size of adsorbent. Powder mordenite had the highest speed of Cs^+ adsorption as compared to the rest particles of mordenite. There was about 93.5% Cs^+ and 98.5% Sr^{2+} decontamination from 60 mg kg^{-1} Cs-and Sr^{2+}-retaining vermiculites respectively. The best effective condition for Cs^+ and Sr^{2+} decontamination using zeolites from vermiculite was found to be use of large vermiculite (> 150 μm), 0.3M KCl extracting solution in coexistence of powder natural mordenite (< 80 μm) using wet sieving direct contact method with horizontal shaking time of 3 h. The direct method was recommended for field testing in the decontamination of radioactive Cs^+ and Sr^{2+} using the actual contaminated agricultural soils from Fukushima.

3.6 Evaluation of radioactive decontamination method using contaminated soil

The results on evaluation of the developed radioactive decontamination method for radioactive soil decontamination are given in Figures 3 and 4. In general, there was radioactive decontamination from the different soil types. The rate of radioactive decontamination was affected by many factors such as soil types (Figure 3) and extracting solution types (Figure 4). There was about 20% decontamination in black soil and about 50% decontamination in the brownish soil. In case of extracting solution type, about 90% of radioactive was decontaminated by tap water with Fe pre-treatment (Figure 4).
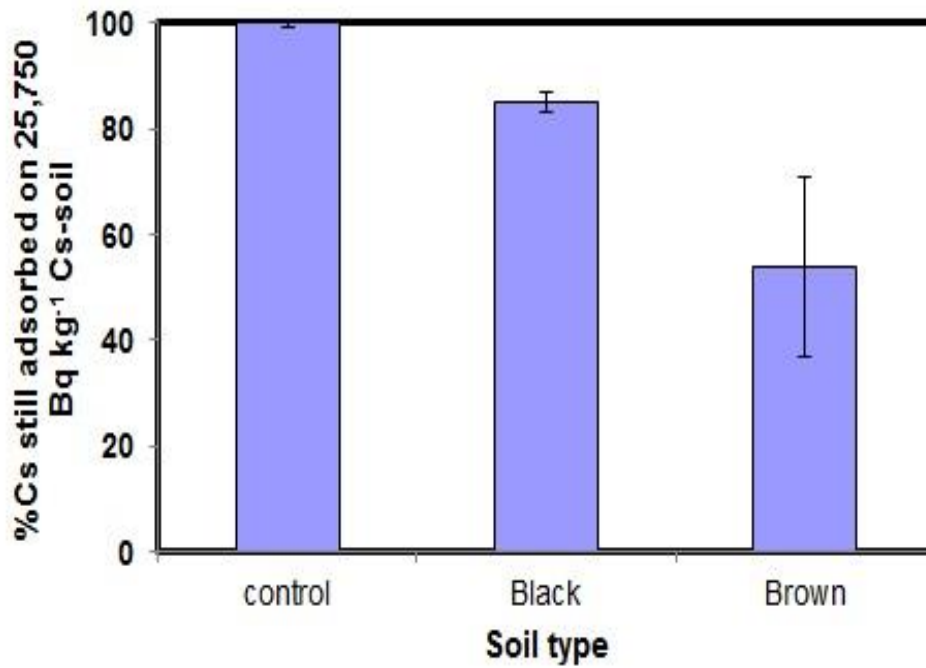
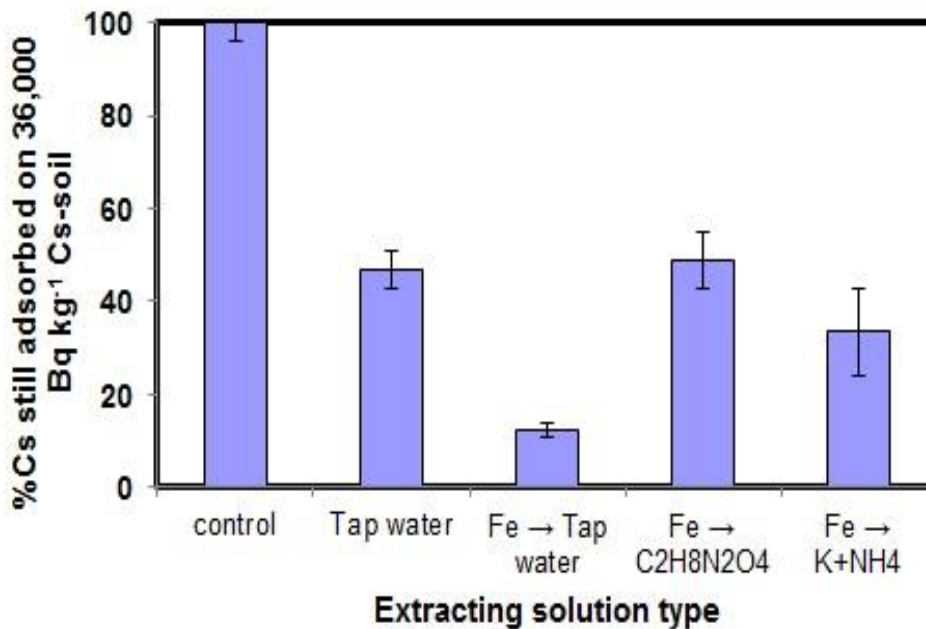**Figure 3.** *Effect of soil type on Cs decontamination from 25,750 Bq kg^{-1} Cs-contaminated Fukushima soil (mordenite - > 150 μm).*

Figure 4. *Effect of Fe(NO$_3$)$_3$ pretreating soil and extracting salt solution type on Cs decontamination from 36,000 Bq kg^{-1} Cs-contaminated Fukushima Soil (0.3 M Mg(NO$_3$)$_2$ pretreated soil; Extracting solution: 0.3 M; soil: 0-90 μm; mordenite: 100-250 μm).*

The method was modified looking at different variables such as soil particles size, type of extracting solution, soil pretreatment and etc. In general, there was an improvement in the rate of radioactive decontamination. Over 90% of Cs^+ were decontaminated when large soil particles (>150 µm) coexisted with small zeolite particles (< 75 µm) and 10-50% when small soil particles (< 150 µm) coexisted with large mordenite particles (> 150 µm) in presence of extracting salt solution depending on soil types. However, the failure of complete radioactive decontamination from most soils was attributed to many factors as discussed in section 3.6.

3.7 Challenges – why a failure of complete Cs decontamination in some soil types?

A failure of complete decontamination of radioactive contamination from certain soil types was due to the reduced effective contact distance between adsorbent and desorbent in the presence of extracting salt solution. The reduced effective contact distance possibly resulted into re-adsorption of radionuclides after desorption by extracting salt from soil. Some of the factors affecting the effective contact distance include:

3.7.1 Reduced surface area

Use of large mordenite resulted into reduced surface area and also sedimentation of mordenite while fine soil particles were evenly dispersed in the extracting salt solution (Plate 1). This phenomenon reduced effective contact distance between soil and zeolite particles in extracting solution i.e. in case of large mordenite versus fine soil particles, it means there was more Cs desorption and re-adsorption on soil clay particles taking place than adsorption on mordenite.
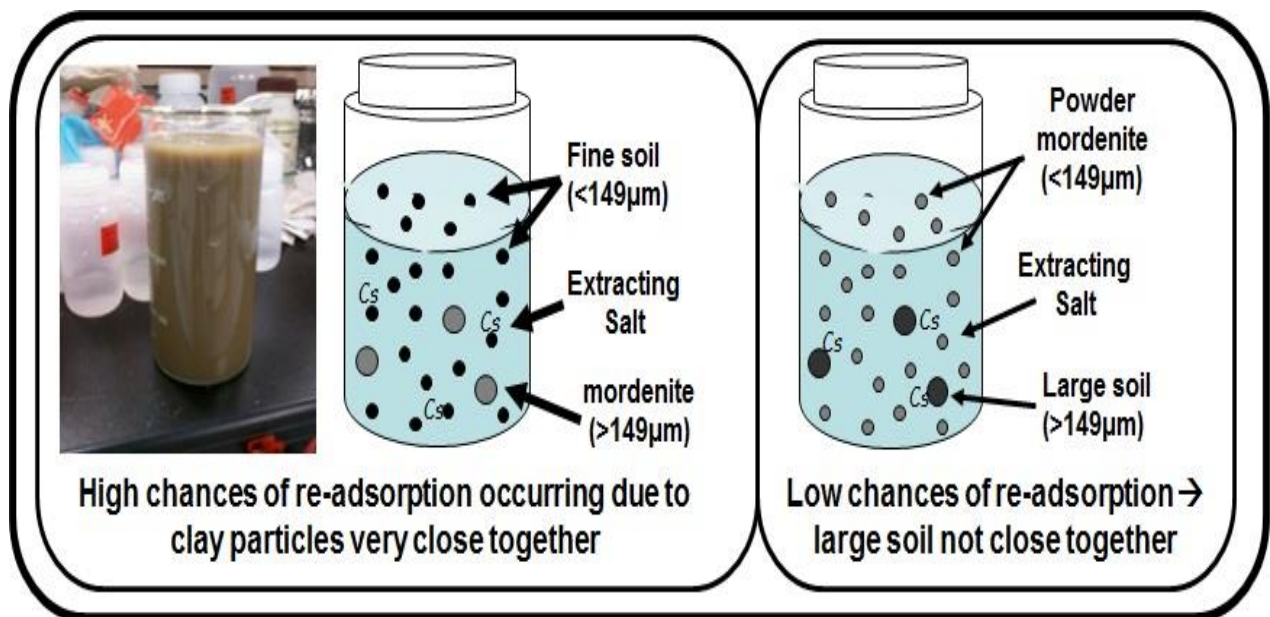

Plate 1. Fine clay particles dispersion in and large mordenite settling down out of the solution

3.7.2 Coating or encapsulation of mordenite by fine clay soil particles

The small soil particles contained very fine clay particles possibly of expanding clays which were very sticky and easily coagulated which resulted in encapsulation of mordenite by soil (plate 2). This observation was common when solid to solution ratio of less than twenty was used. The encapsulation of mordenite possibly blocked Cs adsorption sites on mordenite due to masking effect and also mordenite was not freely in direct contact with the exchangeable cation present in the extracting salt solution. In this case, it is likely that the desorbed Cs from soil in the solution was being re-adsorbed since mordenite was encapsulated and not in direct contact with exchangeable cation. This also explains why there was a failure of complete Cs decontamination from soil types with fine and sticky particles.
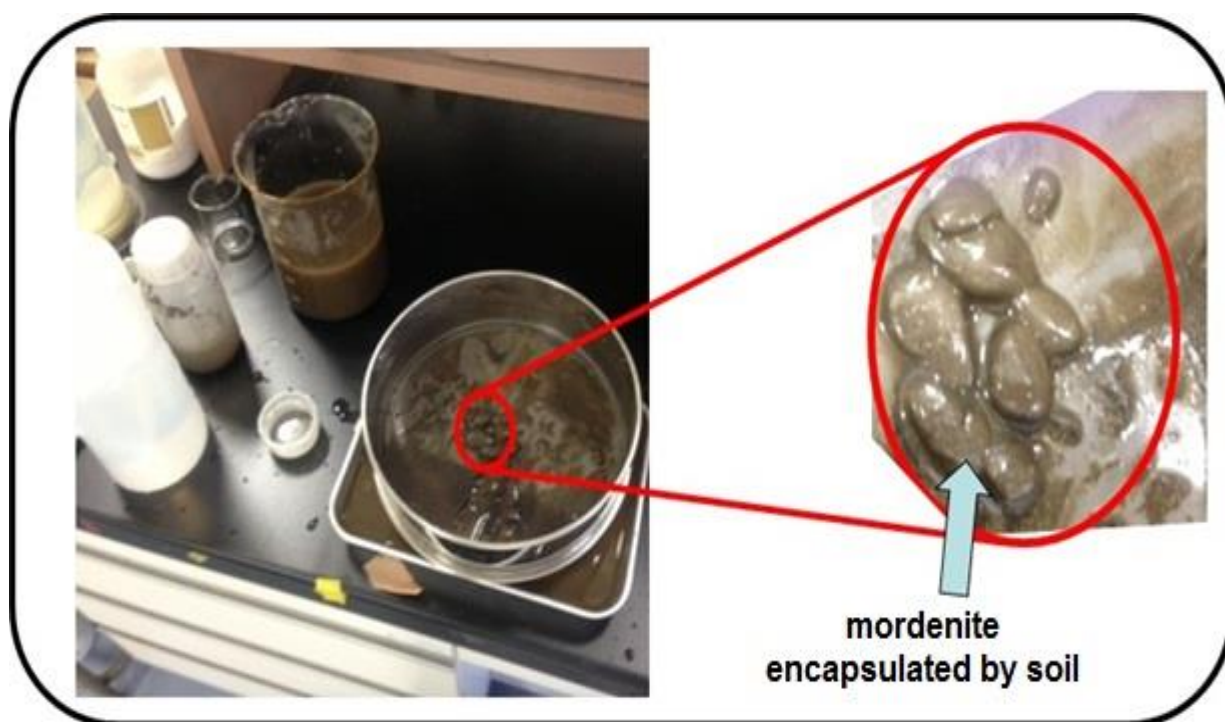

Plate 2. Coating or encapsulation of mordenite by soil particles

3.7.3 Coating of soil and mordenite on the bottle wall

Under low ratio (< 1:15) of solid to solution, some of both coexisting soil and mordenite were being coated on the bottle walls (Plate 3). With changing of the different bottles made of different materials (glass, teflon and polyethylene) the same coating phenomenon still occurred. This removed the solids from the solution and so there was reduced contact between extracting salt solution and soil or mordenite. The efficiency of desorbing Cs from soil by exchanging cation and adsorption of Cs by mordenite was likely reduced. Consequently, this also led to the failure of complete Cs decontamination. However, the coating of soil and mordenite on the bottle wall did not occur when the ratio of solids to solution was more than 20.
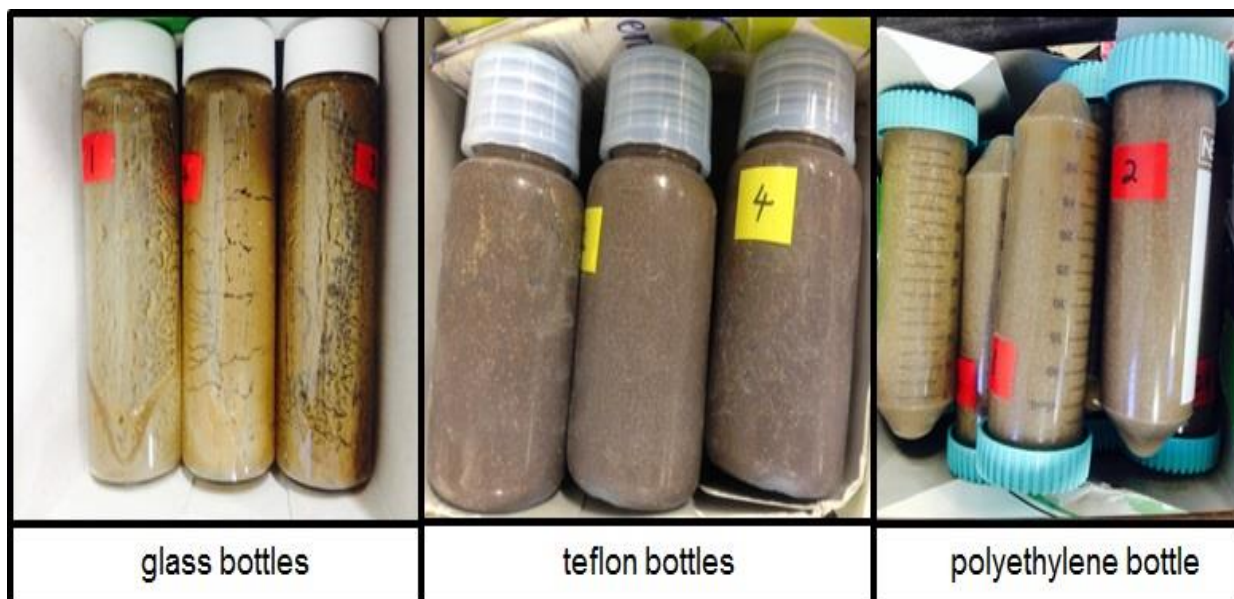
Plate 3. Coating of soil and mordenite on the wall of bottles

3.7.4 High soil electrolyte concentration

There was high electrolyte concentration of already present competing paddy soil K^+ and NH_4^+ due to applied fertilizers. Soils contained much K^+ and NH_4^+ from applied fertilizer i.e. measured radioactive K^+ content was too high in some soils. Use of 0.3 M extracting salt solution of K^+ or NH_4^+ just increased concentration of K^+ and NH_4^+ i.e. from 0.3 M to more than 0.3 M and decreased Cs adsorption selectivity by mordenite when in coexistence with soil. Cesium and Sr adsorption on mordenite decreased with increasing concentration of coexisting cation and cation type. Use of tap water possibly reduces the concentration of soil K^+ and NH_4^+ due to dilution effect which resulted in reduced competition between Cs^+ and K^+ or NH_4^+ for adsorption sites on mordenite.

3.7.5 Cs^+ fixation by clay minerals

The paddy soil contained a lot of mica and vermiculite and since the radioactive decontamination of Fukushima soil happened some more than 4 years ago. It is possible that with time most radioactive Cs was fixed and became difficult to be extracted. This may also explain why there was a failure of complete radioactive decontamination. However, this factor was not examined and it is important to re-examine the phenomenon. This may also require characterization of clay mineralogy of different contaminated soils to know the radionuclides adsorption/desorption behaviour.

3.7.6 Cation competition effect

The cation adsorption selectivity sequence for soil under different concentration of the coexisting cations was not determined as the case for zeolites. It is likely that there was competition effect that affected the adsorption/desorption behaviour on the soil clays. The screening of cation adsorption/desorption selectivity on different soil clays i.e. vermiculite; and etc. and to compare with those cations that have high specific adsorption selectivity by zeolites would help to improve the radioactive decontamination rate.

4.0 Conclusions

In all examined combinations of zeolite species and alkali metal cation species, the amount of adsorption of the alkali metal cations decreased with decreasing pH−pM, due to the adsorption of H^+. The adsorption selectivity of H^+ was affected by both zeolite species and alkali metal cation species. The highest H^+ adsorption selectivity was observed in Rb^+-saturated Linde-type A, and the lowest was observed in Cs^+-saturated mordenite. There was a negative correlation between Si/Al of zeolites and $(pH−pM)_{90}$ value, implying that H^+ selectivity was mainly dependent on the Si/Al ratio and negative charge density of zeolites. Proton adsorption in various zeolites caused the loss of cation retention capacity due to formation of covalent bonding and also could lead to the dissolution of zeolites.

In case of radionuclides decontamination from water, mordenite had the highest Cs^+ adsorption selectivity while Linde-type A had the highest Sr^{2+} adsorption selectivity. The adsorption of Sr^{2+} positively correlated to the CEC values of the zeolites, and Linde-type A with the highest CEC adsorbed more than 99% of Sr^{2+} even in the presence of 0.5 M Na^+ and K^+. In contrast, the CEC values of the zeolites did not relate to the Cs^+ adsorption selectivity.

The decontamination of Cs^+ and Sr^{2+} from Cs- and Sr-retaining vermiculite by washing with 0.3 M KCl was enhanced by the coexistence of mordenite for Cs and Linde-type A for Sr, and more than 90% of Cs^+ and Sr^{2+} were desorbed from vermiculite. In case of radioactive decontamination from soil, there was 95% Cs^+ removed from the Fukushima brownish soil and 40 – 80% Cs^+ removed from other types of Fukushima soils such as black soils. The Cs^+ and Sr^{2+} decontamination from soil were possible due to cation exchange mechanism process. However, the results indicated that possibly other unknown mechanisms also existed that reduced the efficiency of radionuclides removal rate from the contaminated soils during the decontamination process. The failure of complete Cs^+ decontamination in some soils was due to reduced effective contact distance between soil and mordenite in the extracting solution.

5.0 Future targets

In order to achieve complete radioactive Cs^+ and Sr^{2+} decontamination from different soil types under different chemical conditions, the following experimental modifications or improvements are recommended given not in the order of their importance.

16

- To extensively evaluate the effect of solid to solution ratios to find optimum ratio for effective contact distance between soil and mordenite in the extracting salt solution.
- To use non sticky bottle materials to minimize coating of the solid reactants on bottle surface wall especially under low solid to solution ratios.
- To evaluate the effect of temperature of the extracting salt solution on radioactive decontamination.
- To change the concentration of extracting salts from 0.3M to 0.1μM-0.3M of extracting solutions.
- To determine or quantify the amounts or concentration of already existing soil salts such as K^+ and NH_4^+.
- To examine the factors affecting Cs^+ fixation by clay minerals over time.
- To characterize the clay mineralogy of different contaminated soils and their composition ratio. This would help to know or understand their Cs^+ and Sr^{2+} adsorption/desorption behaviour and to optimize their decontamination rates.
- To screen for cation adsorption/desorption selectivity sequences by different soil clays i.e. vermiculite; and etc. and to compare with those that are highly selective by zeolites.
- To use cation saturated zeolites with same cation species of the extracting salt solutions.

（様式５）(Style5)

6.0 List of published papers

1. Moses Wazingwa Munthali, Mohammed Abdalla Elsheikh, Erni Johan and Naoto Matsue. Proton Adsorption Selectivity of Zeolites in Aqueous Media: Effect of Si/Al Ratio of Zeolites. *Molecules*, 19, 20468-20481 (2014)

2. Moses Wazingwa Munthali, Erni Johan and Naoto Matsue. Proton Adsorption Selectivity of Zeolites in Aqueous Media: Effect of Exchangeable Cation Species of Zeolites. *Environments*, 2, 91-104 (2015)

3. Erni Johan, Toshio Yamada, Moses Munthali Wazingwa, Ponyadira Kabwadza-Corner, Hiromichi Aono, Naoto Matsue. Natural zeolites as potential materials for decontamination of radioactive cesium. *Procedia Environmental Sciences* (in press)

4. M. W. Munthali, E. Johan, H. Aono, N. Matsue. Cs^+ and Sr^{2+} adsorption selectivity of zeolites in relation to radioactive decontamination. *Journal of Asian Ceramic Societies* (in press)

5. Moses Wazingwa Munthali, Ponyadira Kabwadza-Corner, Erni Johan, and Naoto Matsue, Decrease in Cation Exchange Capacity of Zeolites at Neutral pH: Examples and Proposals of a Determination Method. *Journal of Materials Science and Chemical Engineering*, 2, 1-5 (2014)

6. Ponyadira Kabwadza-Corner, Moses Wazingwa Munthali, Erni Johan, and Naoto Matsue, Comparative Study of Copper Adsorptivity and Selectivity toward Zeolites, *American Journal of Analytical Chemistry,* 5, 395–405 (2014)

（様式 5 ）(Style5)

7.0 References

Abdel-Rahman, R.O., Ibrahium, H.A., Yung-Tse, H. *Water*, **2011**, *3*, 551-565.

Almutairi, M. T., Mezari, B., Filonenko, A., Magusin, P.C.M.M., Rigutto, M.S., Pidko, E.A. and Hensen, E.J.M. *ChemCatChem,* **2013**, *5*, 452-466.

Alvarez-Ayuso, E., Garcia-Sanchez, A. and Querol, X. *Water Research,* **2003**, *37*, 4855-4862.

Aono, H., Tamura, K., Johan, E., Yamauchi, R., Yamamoto, T., Matsue, N. and Henmi, T. *Chem. Lett.,* **2013**, *42*, 589-591.

Babel, S. and Kurniawan, T.A. *J. Hazard Mater.*, **2003**, *97*, 219-243.

Bailey, S.E, Olin, T.J., Bricka, R,M., Adrian, D.D. *Water Research*, **1999**, *33*, 2469-2479.

Barshad, I. and Kishk, F.M. *Clays Clay Miner.*, **1970**, *18*, 127-137.

Bonelli, B., Civalleri, B., Fubini, B., Ugliengo, P., Areán, C.O. and Garrone, E. *J. Phys. Chem.,* **2000**, *104*, 10978-10988.

Dushenkov, S. *Plant and Soil*, **2003**, *249*, 167-175.

Dyer, A. and Keir, D. *Zeolites,* **1984**, *4*, 215-216.

Dyer, A. Environmental Mineralogy, Cotter-Howells, J.D., Campell, L.S., Valsami-Jones, E. and Batchelder, M. (Eds), *The Mineral Soc. London, Ser.,* **2000**, 319.

El-Naggar, M.R., El-Kamash, A.M., El-Dessouky, I. and Ghonaim, A.K. *J. Hazard. Mater.,* **2008**, *154*, 963-972.

Erdem, E., Karapinar, N. and Donat, R. *J. Colloid Interface Sci*., **2004,** *280*, 309-314.

Gallant, J. and Prakash, A. A Paper Presented at The Canadian Nuclear Society 30th Annual CNS Conference and 33rd CNS/CAN Student Conference, Canada, **2009**.

Garcia-Sosa, I., Solach-Rios, M. and Olguin, M.T. *J. Radioanal Nucl. Chem*., **2003**, *256*, 273-277.

Hiromi, Y. and Masakazi, A. Photofunctional zeolites: synthesis, characterization, photocatalytic reactions, light harvesting. Nova Science publishers, USA, **2000.**

IAEA, Final Report of the International mission on remediation of large contaminated areas off-site the Fukushima Dai-ichi NPP, 7-15 October 2011, NE/NEFW/2011, Japan, **2011**.

Illman, D.L. *Chem. Eng. News.,* **1993**, 9-21.

Irwin R.J., M. VanMouwerik, L. Stevens, M.D. Seese and W. Basham, "Environmental Contaminants Encyclopedia. Distributed within the Federal Government as an Electronic Document (Projected Public Availability on the Internet or NTIS: 1998)'', National Park Service, Water Resources Division, Fort Collins, Colorado, **1997**.

Kabwadza-Corner, P., Munthali, M.W., Johan, E. and Matsue, N. *Amer. J. Analyt. Chem.*, **2014**, *5*, 395-405.

Katada, N., Suzuki, K., Noda, T., Sastre, G. and Niwa, M. *J. Phys. Chem.*, **2009**, *113*, 19208-19217.

Kim, J. *Bull Korean Chem. Soc.,* **2003**, *24*, 1814-1818.

Macaˊsˇek F., Navraˊtil J.D. and Dulanskaˊ S. *Separ. Sc.i Technol.,* **2002**, *37*, 3673-3692.

Munthali M.W., Johan, E. and Matsue, N. *Environments*, **2015**, *2*, 91-104.

（様式 5 ）(Style5)

Munthali, M.W., Elsheik, M.A., Johan, E. and Matsue, N. *Molecules*, **2014**, *19*, 20468-20481.

National Research Council, 1981. Drinking water and health, National Academy Press, volume 4, 189, Washington, DC., **1981**.

Noda, T., Suzuki, K., Katada, N. and Niwa, M. *J. Catalysis*, **2008**, *259*, 203-210.

Sangvanich, T., Sukwarotwat, V., Wiacek, R.J., Grudzienb, R.M., Glen, E., Fryxell, G.E., Addlemanb, R.S., Timchalk, C. and Yantasee, W. *J. Hazard. Mater.,* **2010**, *182*, 225-231.

Santen, A.R.V. and Neurock, M., Molecular Heterogeneous Catalysis: A Conceptual and Computational Approach. John Wiley and Sons 2009/06/10, ISBN: 352760834.

Sastre G., Katada, N. and Niwa, M. *J. Phys. Chem.*, **2010**, *114*, 15424-15431.

Semmens, M.J. and Martin, W.P. *Water Research,* **1988,** *22*, 537-542.

Serykh, A.I. *Micropor. Mesopor. Mat.*, **2005**, *80*, 321-326.

Su, Y., Sridhar, M.B.B., Han, F.X. Monts, D.L. and Diehl, S.V. WM2008 Conference, February 24-28, Phoenix, AZ, **2008.**

Tiwari, D., Prasad, S.K., Yang, J.K., Choi, B.J. and Lee, S.M. *Environ. Eng. Res*. **2006**, *11*, 106-125.

Wilson, E.K. *Chem. Eng. News,* **1997,** *300*, 30*.*

Zheng, J., Aono, T., Uchida, S., Zhang, J. and Honda, M.C., *Geochemical Journal*, **2012**, *46*, 361-369.